CHAPTER 4

EXPERIMENTAL SETUP AND MEASUREMENTS

4.1 OPTICAL PUMPING OF DYE-DOPED POLYMERS

The setup for the optical pumping of dye-doped polymer sample is shown in Fig. 4.1. The dye-doped polymer samples were transversely pumped with a nitrogen laser. A quartz cylindrical lens of focal length $f = 5.5$ cm was used to focus the nitrogen laser beam in line shape onto the surface of the dye-doped polymer sample. In this project, the dye-doped polymer sample was placed within the range of ±1 mm of the focal length of the cylindrical lens. The dye-doped PVA films were allowed to irradiate in superradiant mode; whereas the dye-doped PMMA slabs were placed inside an oscillator which consisted of a flat aluminium back mirror and the end surface of the sample as the output coupler.

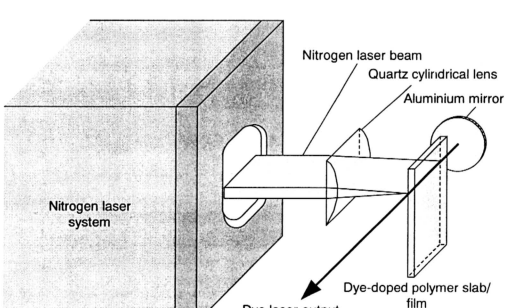

Fig. 4.1 Setup for the optical pumping of dye-doped polymer sample.

Since the dye-doped PVA films were allowed to irradiate in superradiant mode, output laser beams were observed at each end of the dye-doped PVA sample (Fig. 4.2 and 4.3). From each end two beams were detected. The intensities of these four laser beam were almost similar in magnitudes. Therefore, the measurement of the dye laser output will only be fixed on one of the output laser beam (beam ①). The formation of these four output laser beam will be described in detail in Chapter 5.

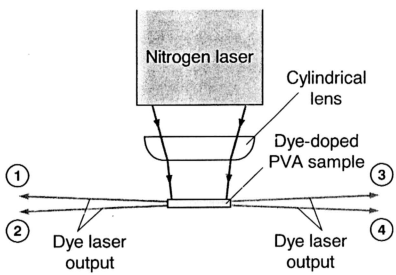

Fig. 4.2 The four output laser beam of dye-doped PVA samples (beam ①, ②, ③ and ④).

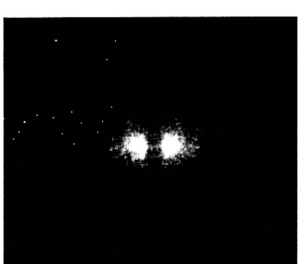

Fig. 4.3 The image of the two output laser beam from one of the output ends of dye-doped PVA sample.

4.2 TRANSVERSELY EXCITED (TE) NITROGEN LASER

A transversely excited (TE) nitrogen laser based on two-stage Blumlein circuit [111, 112] was employed as the pump source of the solid-state dye laser. Fig. 4.4 shows the top-view of the two-stage Blumlein TE nitrogen laser. The laser channel consists of a pair of round-ended brass electrodes (50 cm long, 5 mm thick), separated 15 mm from each other. This configuration contributes a discharge volume of ~ 36 cm^3 (5 × 15 × 480 mm^3). A quartz output window and an aluminium coated mirror were fixed at each end of the cavity. The preionizer which consisted of a linear array of stainless steel blades with tapered ends separated by less than 0.5 mm were placed above the laser channel.

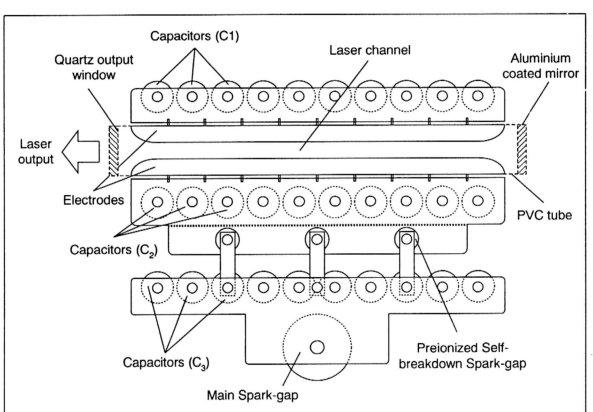

Fig. 4.4 Top-view of the two-stage Blumlein TE nitrogen laser.

The schematic diagram of the two-stage Blumlein circuit is shown in Fig. 4.5. This two-stage Blumlein system was assembled with three capacitors, C_1, C_2 and C_3, each of which is made up of 10 ceramic door-knob type capacitors (Murata Ltd., Japan) each of 1.12 nF, 0.881 nF and 1.92 nF capacitance respectively. Three parallel preionized self-breakdown spark gaps (SG1, SG2 and SG3) were fixed to the system. The delayed breakdowns of these perionized self-breakdown spark gaps enable a large over-voltage across the laser channel to be established. These preionized self-breakdown spark gaps were preionized by small sparks formed between capacitor-coupled pins and one of the laser channel electrodes. This preionization will suppress the breakdown jitters. Thus, a more uniform current distribution was produced, resulting in a more homogeneous discharge excitation of the nitrogen laser.

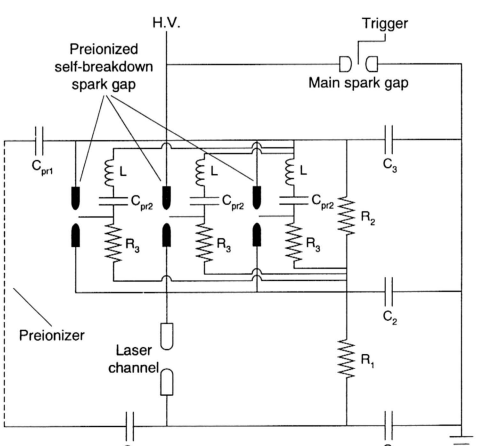

Fig. 4.5 Schematic diagram of the two-stage Blumlein circuit.

The output energy of TE nitrogen laser is controlled by changing the charging voltage and nitrogen gas pressure in the laser channel (Fig. 4.6). Although the TE nitrogen laser system has achieved higher laser output energy at charging voltage of 16 kV and higher gas pressure, however, the plasma discharge along the laser channel becomes non-uniform and the laser output energy fluctuated. Therefore, throughout this project, in order to achieve more uniform discharge along the electrodes of the laser channel, the TE nitrogen laser system was operated at a charging voltage of 15 kV and nitrogen gas pressure of 100 mbar to obtain an output energy of ~ 1 mJ.

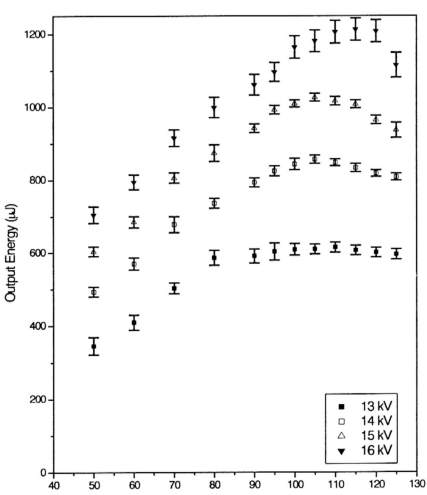

Fig. 4.6 TE nitrogen laser output as a function of nitrogen gas pressure at various charging voltage.

4.3 MEASUREMENT DEVICES

Investigation of the laser radiation of nitrogen laser pumped solid-state dye lasers consists of measuring its output energy, and its laser spectra. The output energy of solid-state dye lasers was measured by using a laser power meter; whereas the laser spectra was detected by using an optical multichannel analyzer (OMA).

4.3.1 Laser Output Energy Measurements

The laser power meter (NOVA, PE-10, Ophir Optronics) used to measure the dye laser output energy was equipped with a pyroelectric-metallic detector head (Fig. 4.7). The laser emission falling onto the detector head produces a temperature gradient along the pyroelectric crystal. This temperature gradient will then generate electric charge, which is proportional to the photon energy absorbed by the detector. The sensitivity of this system is of the order of 0.1 μJ. The EEROM in this system possesses a self-correcting program that ensure accurate readings in the wavelength ranging from 193 nm to 1200 nm.

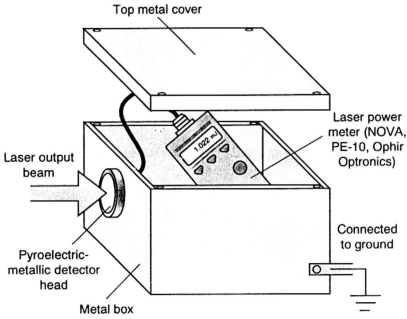

Fig. 4.7 The laser power meter equipped with pyroelectric-metallic detector head was placed inside a grounded metal box.

In this project, the laser pulse length of the energy measurement mode of this detector was set to < 50 μs and the energy range set according to the dye laser output energy. This NOVA system was placed inside a grounded metal box to shield out electromagnetic interference from the nitrogen laser discharge.

4.3.2 Laser Spectra Measurements

The schematic of the setup for solid-state dye laser spectral measurements is shown in Fig. 4.8. A UV-VIS optical fiber was used to guide the dye laser beam into the Optical Multichannel Analyzer (OMA III, EG&G, Princeton Applied Research, model 1461). This OMA system has a 1/8-meter monochromator consisting of an 800 line mm^{-1} grating to disperse the incoming laser beam according to the wavelengths and the intensities of each wavelength are registered by a photodiode array. A neutral density filter was positioned in front of the optical fiber to attenuate strong laser emissions to appropriate intensity levels for the measurements.

The operation of the detector head of the OMA system was controlled by a microcomputer, and this detector head was cooled to $-5^{\circ}C$ by a peltier effect device. The shutter of the photodiode array was set to a 3-second window to ensure the capture of the dye laser pulse. The background dark noise associated with this acquisition time was eliminated by background subtraction.

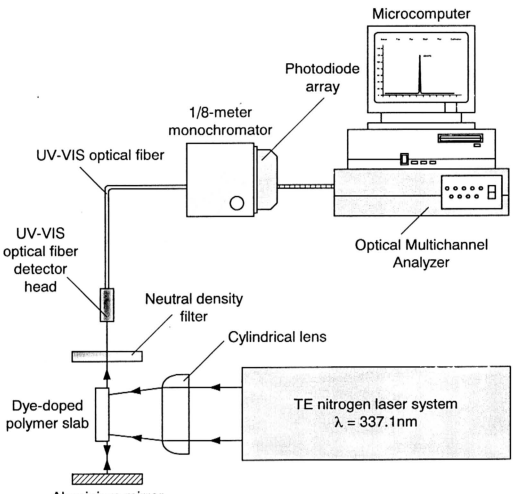

Fig. 4.8 Schematic of the setup for solid-state dye laser spectral measurements.

4.4 DETERMINATION OF REFRACTIVE INDEX AND THICKNESS OF DYE-DOPED THIN FILM

The optical properties of dye-doped polymer cell such as refractive index, thickness *etc.* are important parameters that will affect the optical quality of the cell and the mechanism of energy transfer from pumping light source to the cell. In this project, the refractive indices of dye-doped polymer cells are found to be varying with the dye doping concentrations, and these indices are important parameters in the determination of dye-doped film thickness. Therefore, the determinations of refractive index and film thickness had been carried out in order to monitor the optical quality of the dye-doped polymer cells.

4.4.1 Refractive Index Measurement

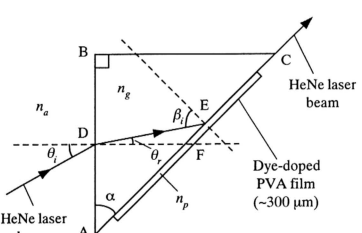

Fig. 4.9 Schematic drawing of the light path from air through a prism to the dye-doped PVA film.

Fig. 4.9 shows the schematic drawing of the light path from air through a prism to the dye-doped PVA film. The dye-doped PVA film of thickness of ~300 μm was directly coated on a surface of a right angle glass prism. An unexpanded beam, from a HeNe laser was incident at an angle θ_i at point D on the first surface (AB) of the prism. At point D,

the beam is refracted at an angle θ_r and incidents at an angle β_i at point E on the glass-film interface (AC) of the prism. From Snell's Law,

$$n_a \sin\theta_i = n_g \sin\theta_r \tag{4.1}$$

where n_a and n_g are refractive index of air and prism respectively. From geometry, with $\angle BAC = \alpha$, and from ΔADF and ΔDEF, we have

$$\beta_i = \theta_r + \alpha \tag{4.2}$$

If β_i is the critical angle of glass-film interface,

$$n_g \sin\beta_i = n_p \tag{4.3}$$

where n_p is the refractive index of the dye-doped PVA film. Substituting Equations (4.1) and (4.3) into Equation (4.2) we have

$$n_p = n_g \sin\left[\sin^{-1}\left(\frac{n_a}{n_g}\sin\theta_i\right) + \alpha\right]. \tag{4.4}$$

From Equation (4.4), by knowing α and n_g, n_p can be obtained by measuring θ_i. For a fixed value of n_p, θ_i is dependent on the choice of α and n_g. Experimentally, θ_i should be as large as possible so that the percentage error incurred in the measurement of θ_i is minimized.

Fig 4.10 shows the dependence of θ_i on α and n_g. It can be seen that θ_i increases as α and n_g approaches 1.5 and 50° respectively. In this work, a right angle prism with angle $\alpha = 45°$ and refractive index $n_g = (1.519 \pm 0.001)$ was chosen in the determination of refractive index n_p of dye-doped PVA films.

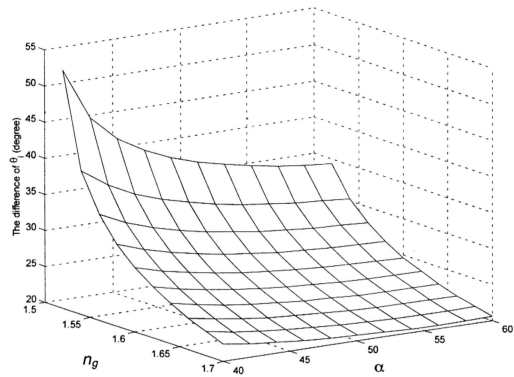

Fig. 4.10 The dependence of θ_i on α and n_g for $1.35 < n_p < 1.50$.

Thus, Equation (4.4) becomes

$$n_p = n_g \sin\left[\sin^{-1}\left(\frac{n_a}{n_g}\sin\theta_i\right) + \frac{\pi}{4}\right] \tag{4.5}$$

This method is also applicable for the determinations of refractive index of dye-doped PMMA slabs. The dye-doped PMMA slab was attached onto the surface of a right angle prism, which index matching fluid ($n \approx 1.5$) was employed as an interfacing medium of prism and dye-doped PMMA slab.

The results of the determination of refractive index of dye-doped PMMA slabs and dye-doped PVA films with different dye concentrations were shown in Chapter 5.

4.4.2 Thickness of the Dye-Doped PVA Films

In this project, the thickness of dye-doped PVA film was estimated by using a Michelson interferometer, instead of the Tolansky method. The Tolansky method can actually be used to measure film thickness that approaches the size of a single atom [118]. However, this method was not suitable for the measurement of the thickness of dye-doped PVA films which are prepared by using the dip-coat method. This was due to the fact that the surface of the dye-doped PVA films prepared by the dip-coat method were uneven. Therefore, the thickness of the dye-doped PVA films had to be estimated by using a Michelson interferometer.

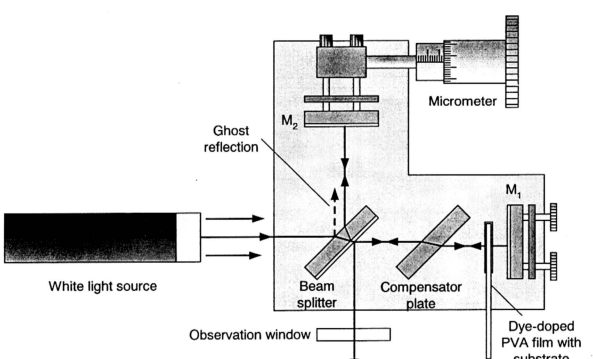

Fig. 4.11 The Michelson interferometer.

Fig. 4.11 shows the experimental arrangement of a Michelson interferometer. A beam of collimated white light, falls onto a beam splitter and is divided into two beams. One beam is transmitted towards mirror M_1; the other proceeds by reflection towards

movable mirror M_2. These waves are reflected at each of these mirrors and are returned along their directions of incidence. Each wave eventually enters the observation window. Thus the two waves are united, and interference can be expected.

Initially, the movable mirror M_2 has to be adjusted to the position d_1 such that an interference occurred for the white light. Upon placing a plain glass substrate in between the compensator plate and mirror M_2, the interference pattern disappears due to the mismatch in optical paths of the two arms of the interferometer. Mirror M_2 has to be adjusted to a new position d_2 such that the interference pattern reappears.

The optical path difference is

$$2(n_g - 1)t_g = 2(d_2 - d_1) \tag{4.6}$$

where n_g is the refractive index of glass substrate and t_g is the thickness of glass substrate.

The plain glass substrate is then removed and is replaced by a dye-doped PVA film coated on a similar glass substrate. The interference pattern again vanishes. Mirror M_2 has to be shifted to another position d_3 in order to recover the interference pattern. This is due to the extra optical path imposed by the dye-doped PVA film. Therefore, the optical path difference now becomes

$$2\left[(n_g - 1)t_g + 2(n_p - 1)t_p\right] = 2(d_3 - d_1) \tag{4.7}$$

where n_p and t_p is the refractive index and thickness of dye-doped PVA film respectively. Thus, from the difference of Equation (4.6) and (4.7), the extra optical path difference contributed by dye-doped PVA film is

$$4(n_p - 1)t_p = 2(d_3 - d_2) \tag{4.8}$$

Thus,

$$t_p = \frac{d_3 - d_2}{2(n_p - 1)} \tag{4.9}$$

The refractive index n_p of the dye-doped PVA film was determined by the method discussed in Section 4.4.1. From Equation (4.9), the thickness of dye-doped PVA film can be determined.

The results of the determination of the thickness of dye-doped PVA films with different dye concentrations are discussed in Chapter 5.